Cellular and Molecular Biology
E-ISSN : 1165-158X / P-ISSN : 0145-5680
www.cellmolbiol.org

Screening of natural products atlas for identification of lead molecule to treat angina pectoris using bioinformatics approaches

Aziz Unnisa[1,*], Suresh B. Jandrajupalli[2], Badria A Elamine[3], Omkalthoum A Mohamed[4], Khetam Saad Alreshidi[5], Aliyah Hamdan Alshammari[5], Hajer shaty Alshammari[5], Norah Bandar[5], Ramana Gangireddy[6]

[1] Department of Pharmaceutical Chemistry, College of Pharmacy, University of Ha'il, Ha'il 81442, Saudi Arabia
[2] Department of Preventive Dental Sciences, College of Dentistry, University of Hail, Ha'il 81442, Saudi Arabia
[3] Department of Radiology, College of Applied Medical Sciences, University of Ha'il, Ha'il 81442, Saudi Arabia
[4] Department of Special Education, College of Education, Hail University, Ha'il, Ha'il 81442, Saudi Arabia
[5] Pharma D, College of Pharmacy, University of Ha'il, Ha'il 81442, Saudi Arabia
[6] Department of Pharmaceutics, KVSR Siddhartha College of Pharmaceutical Sciences, Vijayawada, AP, India

ARTICLE INFO

Original paper

Article history:
Received: May 09, 2023
Accepted: July 08, 2023
Published: August 31, 2023

Keywords:

Chronic heart disease, angiotensin-converting enzymes, angina pectoris, lead identification, drug design

ABSTRACT

Angina pectoris is amongst the most common diseases. There is a scarcity of effective treatments for this disease. As a result, there is a significant clinical and social interest in predicting and developing novel compounds to treat cardiovascular disorders. So, specific natural products have been screened in this study because they have protective effects against angiotensin-converting enzymes. When taken orally, natural products can help protect against or lessen the severity of angina and heart damage. Natural compounds inhibit regulatory enzymes for controlling Angina. For this, we used computational methods such as drug design to identify novel natural compounds against cardiovascular diseases. Drug design via computational methods is gaining popularity as a quick and effective method to identify lead compounds in a shorter time at a low cost. This research work aims to predict novel lead inhibitor compounds against ACE to treat angina pectoris. This would ensure that, in early preclinical studies, there will be lower failure rates due to the demonstrated safety profiles of the predicted compounds.

Doi: http://dx.doi.org/10.14715/cmb/2023.69.8.19

Introduction

Clinically, coronary heart disease can manifest in various ways, including rhythm irregularities, sudden death, pump failure, complete lack of symptoms (silent ischemia), and classic angina (1). Heart attacks can happen following physical or emotional stress and may last for 3 to 5 minutes (2, 3). Additionally, it can lead to uncommon kinds of angina, mostly caused by coronary spasms, such as angina when resting. Angina might gradually get less severe and last for months or even years, but it can sometimes abruptly get worse. This type of angina is known as unstable angina, and since acute myocardial infarctions progress frequently, it is important to identify it as soon as possible (4-6). Asymptomatic coronary heart disease affects 2.5% of males between the ages of 40 and 60. A common finding in individuals with unstable coronary syndromes is silent myocardial ischemia. According to the Framingham Study, patients and doctors failed to recognize 25% of all myocardial infarctions (7, 8). Pharmacological interventions for angina have mostly focused on reducing increases in myocardial oxygen demand by lowering heart rate and systolic blood pressure and/or improving coronary blood flow by relaxing vascular smooth muscle (9, 10). In addition to easing angina symptoms, lowering resting heart rate is a key indicator of a patient's higher risk of adverse outcomes if they have CAD. Beta-adrenergic blockers (BBs), calcium antagonists (CAs, including dihydropyridines and non-dihydropyridines), and nitrates are the most often utilized anti-angina agents (11, 12).

The drug discovery process has been significantly impacted by recent developments in molecular biology, high-throughput crystallization techniques, high-energy synchrotron sources, combinatorial and fragment-based chemistries, and bioinformatics. These developments have given rise to a renewed interest in structure-based drug discovery (13, 14). Although extremely effective, the creation of current-generation ACE inhibitors was the result of serendipity and great discoveries; it was accomplished without the knowledge of the sequence or three-dimensional structure of the enzyme. Somatic ACE is a complicated two-domain enzyme with an N- and a C-domain, each possessing an active site with comparable but different substrate specificities and chloride-activation needs. This fact was only discovered after the development of ACE inhibitors. Therefore, developing domain-selective inhibitors may result in next-generation medications with modified safety and effectiveness profiles (15).

The zinc metallopeptidase ACE, also known as peptidyl-dipeptidase A (EC 3.4.15.1), is a member of the M2 family of the MA clan, which includes all contemporary polypeptides descended from a single ancestral parent. It is a dipeptidyl carboxypeptidase that, in vitro, catalyzes the hydrolytic cleavage of dipeptides from a wide range

* Corresponding author. Email: khushiazeez@yahoo.co.in

of oligopeptides (16, 17). The in vivo conversion of plasma-circulating Ang I (DRVYIHPFHL) into the powerful vasopressor Ang II by removal of the C-terminal His-Leu is its best-known use. Angiotensinogen, a 55-kDa plasma protein produced from the liver, has a Leu10-Val11 peptide link hydrolyzed largely by renin. ACE also influences blood pressure by cleaving bradykinin (BK, RPPGFSPFR), eliminating its vasodilating function. For this reason, ACE is also called kininase II (kininase I being carboxypeptidase N). Plasma kallikrein, a serine proteinase, produces BK from a kininogen precursor in a manner similar to how Ang I is created (18, 19).

Due to their lack of negative side effects, natural products are rapidly gaining favor in treating renal illnesses around the world. These substances are involved in various biological processes (20). For instance, flavonoids, a class of low molecular weight phenolic compounds, are becoming increasingly popular due to the many positive health effects they have and their ability to exert multiple biological properties, including protection from kidney diseases and use in nutraceutical, pharmaceutical, medicinal, and cosmetic applications (21). The most important components of the human diet are flavonoids, which are anti-inflammatory secondary metabolites with a 15-carbon (C6-C3-C6) backbone structure. Various higher plants with red, blue, or purple hues contain flavonoids, which are secondary metabolites with varying phenolic structures (22). Natural products play a crucial role in managing and preventing cardiovascular diseases like angina pectoris because of their effect on immune cell activation, maturation, and signaling transduction, which can inhibit regulatory enzymes or transcription factors that are important for controlling ischemia (23). Therefore, The Natural Product Atlas database has been investigated for its potential anti-inflammatory, antioxidant, anti-cardiovascular, neuroprotective, and strong anticancer effects in a wide range of acute and chronic human disorders (24, 25). We need various methods to assess compounds' biological activity to draw meaningful conclusions. In this study, we'll use a few bioinformatics tools for our investigations (14).

Materials and Methods

Target retrieval from RCSB PDB

The 3D structure of targeted protein angiotensin-converting enzymes (ACE) was downloaded from RCSB PDB by using its specific PDB ID 1O86 (19). PDB, the online internet information portal provides access to 3D structural data of macromolecules (proteins, DNA, and RNA) (26).

Target protein optimization and minimization

MODELLER was used for loop refinement of the target protein (27). Swiss PDB Viewer (28) and RAMPAGE were used to optimize and minimize the protein crystal structure. RAMPAGE created a Ramachandran Plot that revealed no protein conflicts. The plot also shows which residues are in the favored, allowed, and outlier zones(29).

Database preparation

The Natural Products Atlas, a comprehensive database that contains natural compounds, was downloaded from PubChem, and drug-like behavior molecules were chosen using the Lipinski criterion. There were 32552 compounds in all (30).

Pharmacophore modeling and virtual screening

The pharmacophore model was created using the Molecular Operating Environment software. The pharmacophore model was created based on the co-crystallized structure and already reported inhibitors of our target proteins. Virtual screening is a drug discovery technique that searches through libraries of molecules for structures that have the highest probability of binding to a therapeutic target based on distinct descriptors. This was done with MOE software's help against the Natural Product Atlas database (31).

Molecular docking and docking validation

The top 20 compounds from pharmacophore-based virtual screening were chosen after sorting hits by their pharmacophore-fit RMSD score for 1O86. Using AutoDock Vina (32), these top 20 compounds were docked with receptors, and their binding affinities and protein-ligand interactions were analyzed. PyMOL (33) was used to create complex receptor and ligand files, whereas BIOVIA Discovery Studio (34) was applied to find interactions in two dimensions.

The optimal scoring algorithm was employed for high throughput virtual screening to scrutinize the appropriate candidates. The highest-scoring functions were created using a decoy dataset of inactive and active ligands to filter the unidentified compounds. The decoy dataset was created using a Database of Useful Decoys Enhanced (35). The decoys' SMILES were used to create 2D structures of the chosen compounds using Data Warrior (36). The target protein of choice was docked against active and decoy chemicals. The receiver operating characteristic curve (ROC curve) was used to evaluate the dependability of the chosen scoring functions and assign higher points to active ligands over inactive ligands. The ROC curve is calculated using a script written in R (37, 38).

Toxicity analysis

To determine the drug-likeness and toxicity features of compounds, the pkCSM (39) and QikProp developed by Professor William L. Jorgensen (40) were utilized. They are reported as essential and valuable tools for evaluating important druglike descriptors like adsorption, distribution, metabolism, excretion, and toxicity (ADMET). These tools are also employed for predicting lead likeness concerning mutagenicity and carcinogenicity.

Lead identification

Docking score, RMSD values, protein-ligand interactions, lead likeness and drug-likeness analysis, as well as toxicity analysis studies such as Molecular Weight (MW), Hydrogen Bond Donner (HBD), Hydrogen Bond Acceptor (HBA), partial coefficient logP, rings, Polar Surface Area (PSA), rotatable bonds, Blood-Brain Barrier, and Ames Toxicity were used to identify the most active inhibitors. Compounds with the lowest binding affinity, lower RMSD values, the highest lead likeness, and the best interactions were chosen as possible anti-aggregation inhibitors.

MD simulation, PCA and DCCM

Desmond, a software from Schrödinger LLC, was utilized to study 200 ns MD simulations (41). In molecular

dynamics simulation, receptor-ligand docking was the first valuable step because it provides a static view of the molecule's binding position at the protein's active site (42). MD simulations generally predict ligand binding status in the physiological milieu by incorporating Newton's classical equation of motion (43, 44).

Receptor-ligand complex was preprocessed (optimization and minimization) by utilizing Maestro's Protein Preparation Wizard. This step removed steric clashes, bad contacts, and distorted geometries. System Builder tool was employed to build all systems while TIP3P (Intermolecular Interaction Potential 3 Points Transferable), an orthorhombic box, was used as a solvent model with OPLS_2005 force field (45). Counter ions neutralized the models and added 0.15M sodium chloride to simulate physiological conditions with 300K temperature and 1atm pressure throughout the simulation period. Before the simulation, models were loosened. For inspection, trajectories were stored after RMSD confirmed every 100ps, and protein-ligand stability over time. Principal component analysis (PCA) and dynamic cross-correlation matrix (DCCM) were analyzed by using the 'Bio3D' package of R (46).

Molecular mechanics and generalized born surface area (MM-GBSA) calculations

Generalized molecular mechanics During MD simulations of ACE complexed with NPA016099, the Born surface area (MM-GBSA) module of prime was utilized to quantify the binding free energy (Gbind) of the docked complex. The binding free energy was calculated using the OPLS 2005 force field, the VSGB solvent model, and rotamer search methods. The MD trajectory frames were picked at 10 ns intervals following the MD run. Equation 1 was used to compute the total free energy binding.

dGbind=Gcomplex-(Gprotein+Gligand) (1)

Where dGbind = binding free energy, Gcomplex = free energy of the complex, Gprotein = free energy of the target protein, and Gligand = free energy of the ligand.

Results

The 3D structure of the target protein (1O86) was obtained from Protein Data Bank. The total weight of the structure is 68.69 kDa. Its overall symmetry is Asymmetric-C1, and Monomer-A1 is stoichiometry. Figure 1 depicts the protein structure after filling in missing residues, optimization, and minimization, along with the associated Ramachandran plot. The structure's overall quality was 99 percent, with highly preferred observations. In the plot, all other residues are displayed as circles, while glycine is plotted as triangles and proline as squares. The orange areas are the "favored" areas, the yellow areas are the "allowed" areas, and the white areas are the "disallowed" areas.

For the construction of the pharmacophore model via Molecular Operating Environment (MOE), the complex compounds were selected. Figure 2 shows combined pharmacophoric features on the bases of matching properties. Hydrophobic centroids, hydrogen bond acceptors or donors, aromatic rings, cations, and anions are common pharmacophoric characteristics. These pharmacophoric locations can be found either on the ligand itself or they can be projected points in the receptor. For ACE, F1, F3, F4, and F5 stand for a hydrogen bond acceptor, and F2

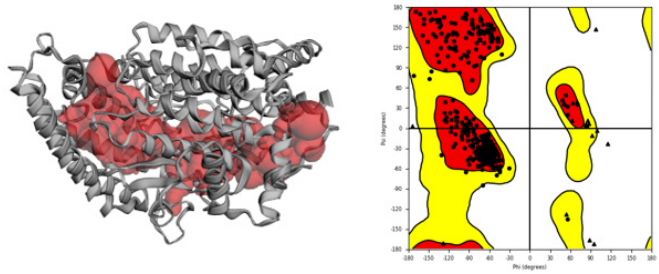

Figure 1. 3D structure of protein retrieved from PDB along with its Ramachandran plot displaying different sections of target protein structure.

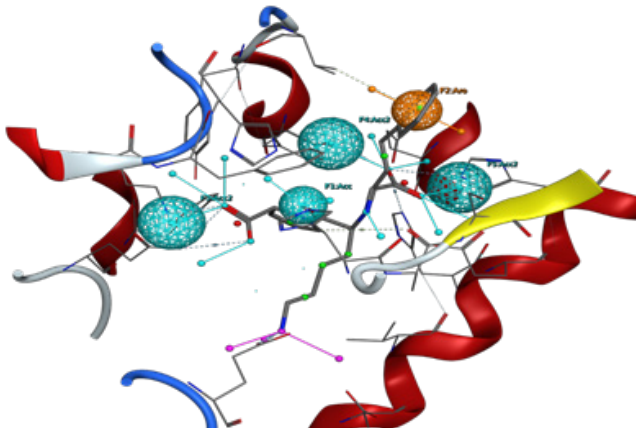

Figure 2. Ligand Based pharmacophore and selected ligand fit on pharmacophore hypothesis.

stands for an aromatic functional group. For virtual screening, The Natural Product Atlas database was utilized after pharmacophore modeling to identify compounds with similar attributes to the pharmacophore model. The Natural Products Atlas was built using FAIR principles (Findable, Accessible, Interoperable, and Reusable) which interlinked with other databases of natural products. A library of 32552 compounds was created using the PubChem data source. The top 20 compounds from pharmacophore-based virtual screening were chosen after sorting 50 hits by their pharmacophore-fit RMSD score for 1O86.

AutoDock Vina performed the docking of the top hits. The study of ADMET (absorption, distribution, metabolism, excretion, and toxicity) was accomplished via QikProp and pkCSM. The top 10 compounds are included in Table 1 based on ADMET and docking findings.

ROC curves were used to construct visual representations of the connection between test specificity and sensitivity candidates. The ROC curves were created by charting the proportion of true positives vs. the percentage of false positives versus the percentage of true negatives (Figure 3).

Following lead identification, one compound (ID: NPA016099) was discovered as the most active of all compounds. Figure 4 depicts the best one's 2D and 3D interactions. The properties of the best one is shown in Table 1. The optimal chemical complex with the protein target was simulated using molecular dynamics for 200 ns. Desmond's simulated trajectories were analyzed. Root-mean-square-deviation (RMSD) and root-mean-square-fluctuation (RMSF) values, as well as protein-ligand interactions, were determined by means of MD trajectory analysis.

Table 1. Table showing ADMET properties, binding affinity, and pharmacophore score of top compounds.

PubChem ID	mol_MW	donorHB	accptHB	QPlogPo/w	QPlogHERG	QPPCaco	QPlogBB	QPlogKhsa	Binding Affinity (Kcal/mol)
NPA010323	956.525	0	27.25	-0.616	-7.855	0.928	-5.541	-1.887	-8.8
NPA010323	956.525	0	27.25	-0.616	-7.854	0.928	-5.541	-1.887	-8.8
NPA014791	996.547	0	27	0.383	-8.634	2.153	-5.001	-1.438	-7.3
NPA016099	440.284	0	11.5	1.086	-6.208	69.872	-2.132	-0.891	-9.3
NPA020704	1020.569	0	24.25	2.471	-8.613	2.829	-5.123	-0.52	-7.8

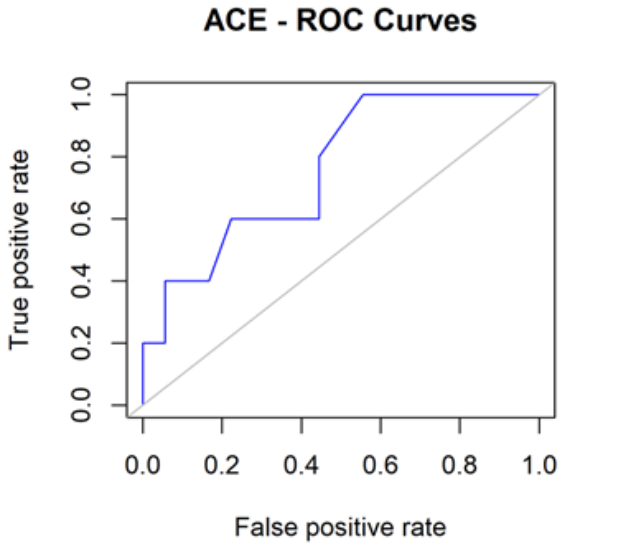

Figure 3. ROC curves of docking validation score.

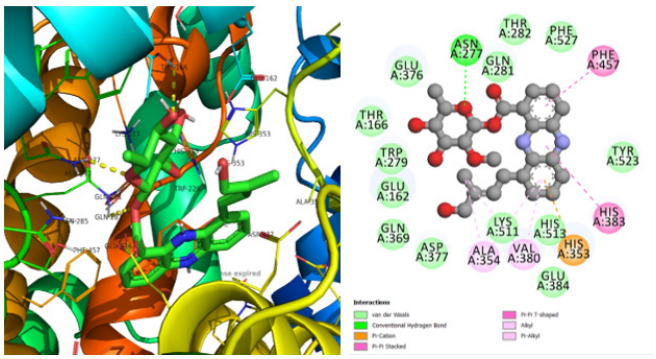

Figure 4. Interactions of the lead compound with protein target showing interacting residues and length of the bond.

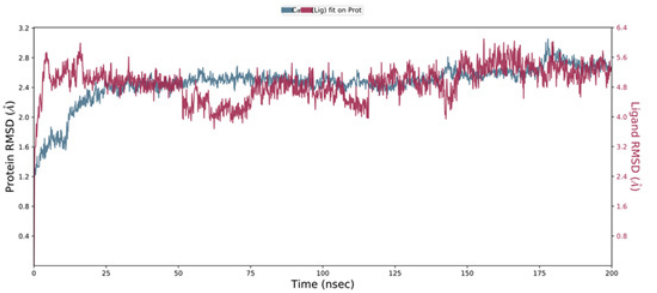

Figure 5. Variation in the root mean square distance (RMSD) between the C-alpha atoms of proteins and ligand (NPA016099-ACE) over time. Protein RMSD shifts over time are plotted on the left Y axis. Differences in ligand root-mean-square distance (RMSD) over time are plotted along the right Y-axis.

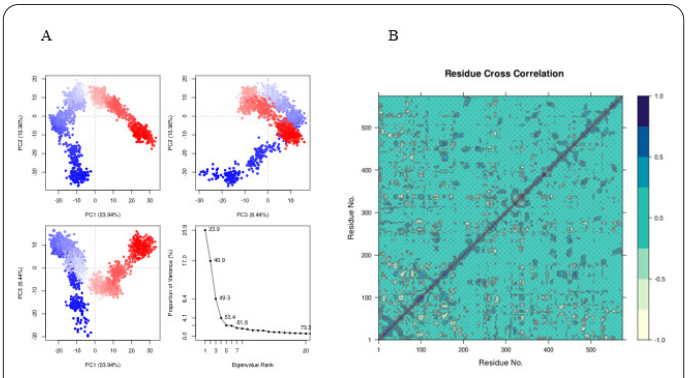

Figure 6.(A) Principal Component Analysis eigenvalue plotted versus the percentage of variance (NPA016099-ACE). The varying areas are displayed in three separate sections. Variations in PC1, PC2, and PC3 add up to 23.94 percent, 16.96 percent, and 8.44 percent, respectively. (B) Complex NPA016099-ACE dynamic cross-correlation map. The residues' positive and negative correlations are depicted by cyan and purple, respectively.

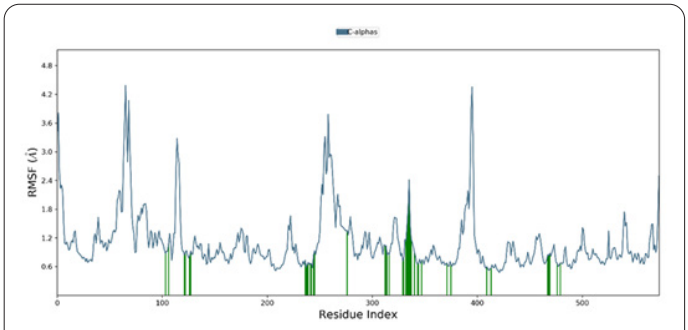

Figure 7. Residue-wise Root Mean Square Fluctuation (RMSF) of protein complexed with ligand.

Figure 5 shows the time-dependent increase in RMSD values for C-alpha atoms in ligand-bound proteins. The RMSD plot shows that the complexed NPA016099-ACE protein stabilized at 20 ns. Once the equilibrium is achieved, the RMSD stays in the range of 1.5 Angstrom for the rest of the run, which is fine.

Protein dynamics are characterized by Principal Component Analysis (PCA) (47). Observing collective trajectory motions during MD simulations is a valuable tool. Graph of eigenvalues (protein) vs. eigenvector index (eigenmode) for the first 20 modes of motion (NPA016099-ACE) (Figure 6:A). NPA016099 and the ACE protein were shown to be significantly correlated with one another, as seen by their high pairwise cross-correlation coefficient value on the cross-correlation map (Figure 6B).

Figure 7 depicts the RMSF value of the ligand-coupled protein. Based on MD trajectories, we know that residues with higher peaks are located in loop regions or N- and C-

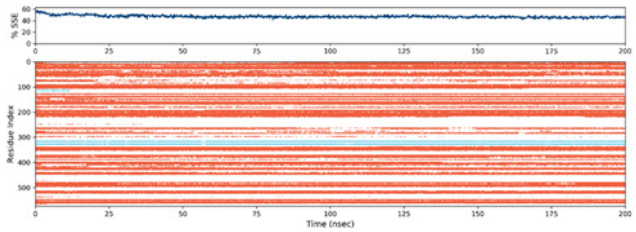

Figure 8. Elements of Protein Secondary Structure are dispersed across protein-ligand complexes with respect to residue index. The alpha helices are represented by the red columns, and the beta strands by the blue ones.

terminal zones (Figure 8).

In Figure 9, it is clear that hydrogen bonds constitute the vast majority of the important ligand-protein interactions established by MD. Hydrogen bonding is especially crucial for the amino acids GLU_162, ASN_277, THR_282, GLU_376, GLU_384, and GLU_441.

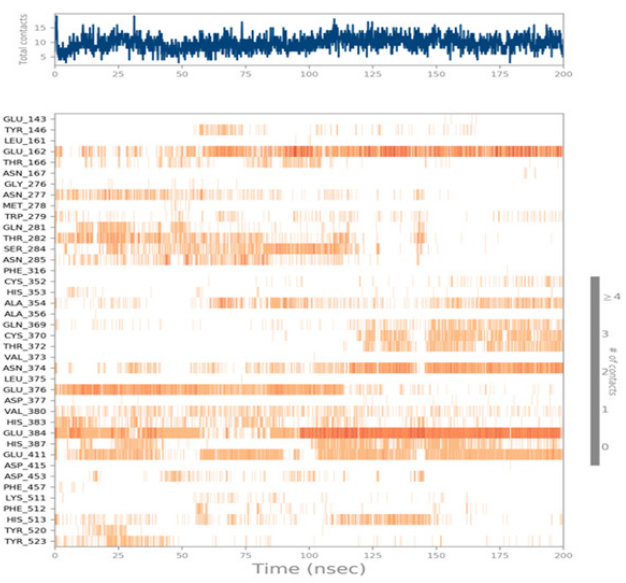

Figure 9. Protein-ligand contact heatmap throughout the trajectory.

Discussion

Natural products play a crucial role in managing and preventing cardiovascular diseases like angina pectoris because of their effect on immune cell activation, maturation, and signaling transduction, which can inhibit regulatory enzymes or transcription factors that are important for controlling ischemia (23). In this study, we used a few bioinformatics tools for our investigations on the Natural Product Atlas database to find lead compounds and draw meaningful conclusions on their biological activity as a potential anti-Angina agent.

The 3D structure of the target protein (1O86) was obtained from Protein Data Bank. The total weight of the structure is 68.69 kDa. For the construction of the pharmacophore model via Molecular Operating Environment (MOE), the complex compounds were selected. Combined pharmacophoric features were determined. Hydrophobic centroids, hydrogen bond acceptors or donors, aromatic rings, cations, and anions are common pharmacophoric characteristics. These pharmacophoric locations can be found either on the ligand itself or they can be projected points in the receptor. For ACE, F1, F3, F4, and F5 stand for a hydrogen bond acceptor, and F2 stands for an aromatic functional group.

For virtual screening, The Natural Product Atlas database was utilized after pharmacophore modeling to identify compounds with similar attributes to the pharmacophore model. The Natural Products Atlas was built using FAIR principles which interlinked with other databases of natural products. A library of 32552 compounds was created using the PubChem data source. The top 20 compounds from pharmacophore-based virtual screening were chosen after sorting 50 hits by their pharmacophore-fit RMSD score for 1O86.

AutoDock Vina performed the docking of the top hits. The study of ADMET (absorption, distribution, metabolism, excretion, and toxicity) was accomplished via QikProp and pkCSM. The top 10 compounds are included in Table 1 based on ADMET and docking findings.

In Table 1, mol_MW represents the molecular weight, which should be between 130.0 and 725.0, and donorHB is the projected number of hydrogen bonds that the solute would give to water molecules. accptHB, the projected number of hydrogen bonds the solute would accept from water molecules in an aqueous solution, can be a non-integer value with a recommended range of 0.0 - 6.0. This is because the value is an average across several different configurations. Given that values are calculated as an average over multiple states, they may not all be integers. It operates between 2.0 and 20.0. The Octanol/water partition coefficient, estimated to be -2.0 to 6.5, is denoted as QPlogPo/w. QPlogHER, Value of the inhibitory concentration (IC50) for the blockade of HERG K+ channels. Negative values below -5 are the cause for alarm. QPPCaco Caco-2 cell permeability prediction, expressed as a number of nanometers per second. The gut-blood barrier can be mimicked using Caco2 cells. The results of QikProp are for passive transport only. In the range of 0–25, consider it poor, and anything beyond 500 is excellent. QPlogBB Expected brain/blood separation ratio. Dopamine and serotonin, for instance, are CNS-negative because they are too polar to cross the blood-brain barrier, with predicted ranges of - 3.0 to - 1.2 when using QikProp to predict orally administered drugs. QPlogKhsa and Human serum albumin binding predictions range from -1.5 to 1.5.

The proposed ROC curves pattern was used to validate the compounds chosen for molecular docking investigations, ensuring that the compounds chosen are active ligands rather than inactive ligands (decoys). It was also discovered that the planned pattern examined active ligands from the top-rated compounds in the chosen database. The area under the curve was 0.761 (Figure 3).

Following lead identification, one compound (ID: NPA016099) was discovered as the most active of all compounds. Figure 4 depicts the best one's 2D and 3D interactions. The properties of the best one is shown in Table 1. The optimal chemical complex with the protein target was simulated using molecular dynamics for 200 ns. Desmond's simulated trajectories were analyzed.

The protein structure (PDB ID: 1o86) is shown to have an increasing RMSD at the same pace and with very little variation. The experiment validated the general belief that the building was sturdy. Ligand fit on protein got equilibrium at 10 ns. After that, throughout the simulation, there was no significant change in the Ligand Fit to Protein.

The RMSD numbers would fluctuate suddenly, sometimes going up and sometimes down. After equilibrium was reached, there was no change in the ligand's RMSD.

Protein dynamics are characterized by PCA (Principal Component Analysis) (47). Observing collective trajectory motions during MD simulations is a valuable tool. Graph of eigenvalues (protein) vs. eigenvector index (eigenmode) for the first 20 modes of motion (NPA016099-ACE) (Figure 6:A). The eigenvalues depict hyperspace eigenvector fluctuations. In simulations, eigenvectors with higher eigenvalues regulate the proteins' total mobility. The top five eigenvectors in our systems showed dominant movements and had larger eigenvalues (23.9-61.8%) than the other eigenvectors, which had low eigenvalues. More than 50% of all changes were covered by the first three PCs (PC1, PC2, and PC3) that were plotted. According to the Figure 6A plots, PC1 clusters had the largest variability (23.94 %), PC2 showed variability (16.96 %), and PC3 had the lowest variability (8.44 %). As a result of its low variability, PC3 has a more compact structure than PC1 and PC2 and is thought to have the most stabilized protein-ligand binding. Simple clustering in the PC subspace revealed conformational variations across all groups, with blue exhibiting the most significant mobility, white indicating intermediate movement, and red indicating less flexibility.

NPA016099 and the ACE protein were shown to be significantly correlated with one another, as seen by their high pairwise cross-correlation coefficient value on the cross-correlation map (Figure 6B). Magenta represents anti-correlated residues (-0.4), whereas cyan represents correlated residues (>0.8). It is clear from a large number of pairwise correlated residues between the protein and ligand that their binding connection is stable.

The stability of ligand binding to the protein is shown by low RMSF values of binding site residues. The secondary structure features such as alpha-helices and beta-strands, are tracked throughout the simulation (SSE). In the graph below, SSE is plotted against the residue index to display its distribution across the protein structure. Totaling 47.20 percent, it was found that helix made up 45.78 percent, and strand made up 1.42 percent.

The ligand-protein interaction can be monitored over the course of the simulation, in accordance with the chart below. The contacts and interactions (H-bonds, hydrophobic, ionic, and water bridges) discussed on the preceding page are visualized in a timeline on this page. At the top, we may count how many distinct times the protein and ligand interact. The panel on the bottom displays, for each frame of the trajectory, which residues are interacting with the ligand. Some residues, shown in a darker orange, make many independent interactions with the ligand, as indicated by the scale on the plot's right.

From Figure 9, it is clear that hydrogen bonds constitute the vast majority of the important ligand-protein interactions established by MD. Hydrogen bonding is especially crucial for the amino acids GLU_162, ASN_277, THR_282, GLU_376, GLU_384, and GLU_441.

Drug development has been studied extensively because of the potential for transdisciplinary strategies to speed up the process and reduce overall costs. The primary objective of this research was to explore target proteins for angina pectoris so that a lead drug could be selected for them. To counteract the effects of natural products on the ACE protein, we chose substances that have this property. An artificially synthesized inhibitor, identified by the NPA016099, blocks the action of 1O86 at its receptor. We reasoned that this material could serve as a starting point for the development of a medication that targets angina pectoris selectively without affecting other cellular processes. These results will be useful to researchers and may lead to the development of a new medicine for the treatment of angina pectoris.

Acknowledgments
The authors are thankful to the scientific research deanship at the University of Hail-Saudi Arabia for providing us the funding through project number RG 21015.

Interest conflict
The authors declare no conflict of interest.

Consent for publications
All the authors read and approved the final manuscript for publication.

Availability of data and material
All data generated during this study are included in this published article

Authors' Contribution
All authors had equal roles in study design, work, statistical analysis and manuscript writing.

Funding
This research has been funded by the scientific research deanship at the University of Hail-Saudi Arabia through project number RG 21015

Ethics approval and consent to participate
No humans or animals were used in the present research.

References

1. Sterz H, Koller H, Kobinia G. Angina pectoris. Wien Med Wochenschr 1988;138(15-16):369-373.
2. Cohn PF. Silent ischemia: a timely aspect in coronary artery disease. Herz 1987;12(5):314-317.
3. Wilhelmsen L, Rosengren A, Hagman M, Lappas G. Prognosis is often poor in chest pain not interpreted as angina pectoris. Simultaneous occurrence of cardiovascular risk factors increases the risk of premature death. Lakartidningen 2000;97(9):976-978.
4. Munger TM, Oh JK. Unstable angina. Mayo Clin Proc 1990;65(3):384-406.
5. Brann WM, Tresch DD. Management of stable & unstable angina in elderly patients. Compr Ther 1997;23(1):49-56.
6. Shub C. Stable angina pectoris: 1. Clinical patterns. Mayo Clin Proc 1990;65(2):233-42.
7. von Arnim T. Clinical importance of silent ischemia. Z Kardiol 1992;81(4):188-92.
8. Zuchi C, Tritto I, Ambrosio G. Angina pectoris in women: focus on microvascular disease. Int J Cardiol 2013;163(2):132-140.
9. Elgendy IY, Winchester DE, Pepine CJ. Experimental and early investigational drugs for angina pectoris. Expert Opin Investig Drugs 2016;25(12):1413-1421.
10. Gupta AK, Winchester D, Pepine CJ. Antagonist molecules in the treatment of angina. Expert Opin Pharmacother 2013;14(17):2323-2342.

11. Kolloch R, Legler UF, Champion A, Cooper-Dehoff RM, Handberg E, Zhou Q, et al. Impact of resting heart rate on outcomes in hypertensive patients with coronary artery disease: findings from the International VErapamil-SR/trandolapril STudy (INVEST). Eur Heart J 2008;29(10):1327-1334.
12. Task Force M, Montalescot G, Sechtem U, Achenbach S, Andreotti F, Arden C, et al. 2013 ESC guidelines on the management of stable coronary artery disease: the Task Force on the management of stable coronary artery disease of the European Society of Cardiology. Eur Heart J 2013;34(38):2949-3003.
13. Blundell TL, Jhoti H, Abell C. High-throughput crystallography for lead discovery in drug design. Nat Rev Drug Discov 2002;1(1):45-54.
14. Iqbal MN, Rasheed MA, Awais M, Chammam W, Kanwal S, Khan SU, et al. BMT: Bioinformatics mini toolbox for comprehensive DNA and protein analysis. Genomics 2020;112(6):4561-4566.
15. Turner AJ, Hooper NM. The angiotensin-converting enzyme gene family: genomics and pharmacology. Trends Pharmacol Sci 2002;23(4):177-183.
16. Acharya KR, Sturrock ED, Riordan JF, Ehlers MR. Ace revisited: a new target for structure-based drug design. Nat Rev Drug Discov 2003;2(11):891-902.
17. Soubrier F, Alhenc-Gelas F, Hubert C, Allegrini J, John M, Tregear G, Corvol P. Two putative active centers in human angiotensin I-converting enzyme revealed by molecular cloning. Proc Natl Acad Sci USA 1988;85(24):9386-90.
18. Wei L, Alhenc-Gelas F, Corvol P, Clauser E. The two homologous domains of human angiotensin I-converting enzyme are both catalytically active. J Biol Chem 1991;266(14):9002-9008.
19. Natesh R, Schwager SL, Sturrock ED, Acharya KR. Crystal structure of the human angiotensin-converting enzyme-lisinopril complex. Nature 2003;421(6922):551-554.
20. Atanasov AG, Zotchev SB, Dirsch VM, Orhan IE, Banach M, Rollinger JM, et al. Natural products in drug discovery: advances and opportunities. Nat Rev Drug Discov 2021;20(3):200-216.
21. Panche AN, Diwan AD, Chandra SR. Flavonoids: an overview. J Nutr Sci 2016;5:e47.
22. Cao YL, Lin JH, Hammes HP, Zhang C. Flavonoids in Treatment of Chronic Kidney Disease. Molecules 2022;27(7):2365
23. Ginwala R, Bhavsar R, Chigbu DI, Jain P, Khan ZK. Potential Role of Flavonoids in Treating Chronic Inflammatory Diseases with a Special Focus on the Anti-Inflammatory Activity of Apigenin. Antioxidants (Basel) 2019;8(2):35.
24. Kopustinskiene DM, Jakstas V, Savickas A, Bernatoniene J. Flavonoids as Anticancer Agents. Nutrients 2020;12(2):457.
25. Serafini M, Peluso I, Raguzzini A. Flavonoids as anti-inflammatory agents. Proc Nutr Soc 2010;69(3):273-278.
26. Berman HM, Westbrook J, Feng Z, Gilliland G, Bhat TN, Weissig H, et al. The Protein Data Bank. Nucleic Acids Res 2000;28(1):235-242.
27. Eswar N, Webb B, Marti-Renom MA, Madhusudhan MS, Eramian D, Shen MY, et al. Comparative protein structure modeling using Modeller. Curr Protoc Bioinformatics 2006;Chapter 5:Unit-5 6.
28. Guex N, Peitsch MC. SWISS-MODEL and the Swiss-PdbViewer: an environment for comparative protein modeling. Electrophoresis 1997;18(15):2714-2723.
29. Ho BK, Brasseur R. The Ramachandran plots of glycine and preproline. BMC Struct Biol. 2005;5:14.
30. van Santen JA, Jacob G, Singh AL, Aniebok V, Balunas MJ, Bunsko D, et al. The Natural Products Atlas: An Open Access Knowledge Base for Microbial Natural Products Discovery. ACS Cent Sci 2019;5(11):1824-1833.
31. ULC CCG. Molecular Operating Environment (MOE): 1010 Sherbooke St. West, Suite #910, Montreal, QC, Canada, H3A 2R7, 2022; 2015
32. Trott O, Olson AJ. AutoDock Vina: improving the speed and accuracy of docking with a new scoring function, efficient optimization, and multithreading. J Comput Chem 2010;31(2):455-461.
33. Mura C, McCrimmon CM, Vertrees J, Sawaya MR. An introduction to biomolecular graphics. PLoS Comput Biol 2010;6(8):e1000918.
34. Systèmes D. BIOVIA Discovery Studio. San Diego. 2022.
35. Mysinger MM, Carchia M, Irwin JJ, Shoichet BK. Directory of Useful Decoys, Enhanced (DUD-E): Better Ligands and Decoys for Better Benchmarking. J Med Chem 2012;55(14):6582-6594.
36. Sander T, Freyss J, von Korff M, Rufener C. DataWarrior: An Open-Source Program For Chemistry Aware Data Visualization And Analysis. Journal of Chemical Information and Modeling. 2015;55(2):460-73.
37. Empereur-Mot C, Guillemain H, Latouche A, Zagury JF, Viallon V, Montes M. Predictiveness curves in virtual screening. Journal of cheminformatics. 2015;7:52.
38. Carmona SR. How to calculate ROC curves 2013 [Available from: http://www.ub.edu/cbdd/?q=content/how-calculate-roc-curves.
39. Pires DE, Blundell TL, Ascher DB. pkCSM: Predicting Small-Molecule Pharmacokinetic and Toxicity Properties Using Graph-Based Signatures. J Med Chem 2015;58(9):4066-4072.
40. Laoui A, Polyakov VR. Web services as applications' integration tool: QikProp case study. J Comput Chem 2011;32(9):1944-1951.
41. Bowers KJaC, David E. and Xu, Huafeng and Dror, Ron O. and Eastwood, Michael P. and Gregersen, Brent A. and Klepeis, John L. and Kolossvary, Istvan and Moraes, Mark A. and Sacerdoti, Federico D. and Salmon, John K. and Shan, Yibing and Shaw, David E. Scalable Algorithms for Molecular Dynamics Simulations on Commodity Clusters: IEEE 2006. 43- p.
42. Ferreira LG, Dos Santos RN, Oliva G, Andricopulo AD. Molecular docking and structure-based drug design strategies. Molecules 2015;20(7):13384-13421.
43. Hildebrand PW, Rose AS, Tiemann JKS. Bringing Molecular Dynamics Simulation Data into View. Trends Biochem Sci 2019;44(11):902-913.
44. Rasheed MA, Iqbal MN, Saddick S, Ali I, Khan FS, Kanwal S, et al. Identification of Lead Compounds against Scm (fms10) in Enterococcus faecium Using Computer Aided Drug Designing. Life (Basel) 2021;11(2).
45. Shivakumar D, Williams J, Wu Y, Damm W, Shelley J, Sherman W. Prediction of Absolute Solvation Free Energies using Molecular Dynamics Free Energy Perturbation and the OPLS Force Field. J Chem Theory Comput 2010;6(5):1509-1519.
46. Grant BJ, Skjaerven L, Yao XQ. The Bio3D packages for structural bioinformatics. Protein Sci 2021;30(1):20-30.
47. David CC, Jacobs DJ. Principal component analysis: a method for determining the essential dynamics of proteins. Methods Mol Biol 2014;1084:193-226.